Mapping the transverse coherence of the self amplified spontaneous emission of a free-electron laser with the heterodyne speckle method

Matteo D. Alaimo,[1,7] Maria Pia Anania,[2] Marcello Artioli,[3] Alberto Bacci,[1] Marco Bellaveglia,[2] Franco Ciocci,[3] Enrica Chidroni,[2] Alessandro Cianchi,[4] Giuseppe Dattoli,[3] Giampierro Di Pirro,[2] Massimo Ferrario,[2] Giancarlo Gatti,[2] Luca Giannessi,[3,8] Michele Manfredda,[1,8,*] Roberta Martucci,[1] Andrea Mostacci,[5] Bruno Paroli,[1] Alberto Petralia,[3] Vittoria Petrillo,[1] Riccardo Pompili,[4] Marco A.C. Potenza,[1] Marcello Quattormini,[3] Julietta Rau,[6] Daniele Redoglio,[1] Andrea R. Rossi,[1] Luca Serafini,[1] Vincenzo Surrenti,[3] Amalia Torre,[3] Cristina Vaccarezza,[2] and Fabio Villa[2]

[1]Università degli Studi di Milano and INFN-Mi,Via Celoria, 16 20133 Milano, Italy
[2]INFN-LNF, Via E. Fermi, 40 00044 Frascati, Roma, Italy
[3]ENEA C.R. Frascati, Via E. Fermi,45 00044 Frascati, Roma, Italy
[4] Università di Roma Tor Vergata and INFN, Via della Ricerca Scientifica,1 00133 Roma, Italy
[5]Universita` La Sapienza di Roma and INFN-Roma I, Via Antonio Scarpa 14, Roma, Italy
[6]ISM-CNR Via del Fosso del Cavaliere,100 00133 Roma, Italy
[7]Dipartimento di Chimica, Materiali e Ingegneria Chimica, Politecnico di Milano, 20133 Milano, Italy
[8]Sincrotrone Trieste S.C.p.A., Area Science Park, S.S. 14 Km 163.5, I-34149 Trieste, Italy
[*]Manfredda@gmail.com

Abstract: The two-dimensional single shot transverse coherence of the Self-Amplified Spontaneous Emission of the SPARC_LAB Free-Electron Laser was measured through the statistical analysis of a speckle field produced by heterodyning the radiation beam with a huge number of reference waves, scattered by a suspension of particles. In this paper we report the measurements and the evaluation of the transverse coherence along the SPARC_LAB undulator modules. The measure method was demonstrated to be precise and robust, it does not require any a priori assumptions and can be implemented over a wide range of wavelengths, from the optical radiation to the x-rays.

OCIS codes: (030.1640) Coherence; (030.6140) Speckle.

References and links

1. W. Ackermann, G. Asova, V. Ayvazyan, A. Azima, N. Baboi, J. Bähr, V. Balandin, B. Beutner, A. Brandt, A. Bolzmann, R. Brinkmann, O. I. Brovko, M. Castellano, P. Castro, L. Catani, E. Chiadroni, S. Choroba, A. Cianchi, J. T. Costello, D. Cubaynes, J. Dardis, W. Decking, H. Delsim-Hashemi, A. Delserieys, G. Di Pirro, M. Dohlus, S. Düsterer, A. Eckhardt, H. T. Edwards, B. Faatz, J. Feldhaus, K. Flöttmann, J. Frisch, L. Fröhlich, T. Garvey, U. Gensch, Ch. Gerth, M. Görler, N. Golubeva, H.-J. Grabosch, M. Grecki, O. Grimm, K. Hacker, U. Hahn, J. H. Han, K. Honkavaara, T. Hott, M. Hüning, Y. Ivanisenko, E. Jaeschke, W. Jalmuzna, T. Jezynski, R. Kammering, V. Katalev, K. Kavanagh, E. T. Kennedy, S. Khodyachykh, K. Klose, V. Kocharyan, M. Körfer, M. Kollewe, W. Koprek, S. Korepanov, D. Kostin, M. Krassilnikov, G. Kube, M. Kuhlmann, C. L. S. Lewis, L. Lilje, T. Limberg, D. Lipka, F. Löhl, H. Luna, M. Luong, M. Martins, M. Meyer, P. Michelato, V. Miltchev, W. D. Möller, L. Monaco, W. F. O. Müller, O. Napieralski, O. Napoly, P. Nicolosi, D. Nölle, T. Nuñez, A. Oppelt, C. Pagani, R. Paparella, N. Pchalek, J. Pedregosa-Gutierrez, B. Petersen, B. Petrosyan, G. Petrosyan, L. Petrosyan, J. Pflüger, E. Plönjes, L. Poletto, K. Pozniak, E. Prat, D. Proch, P. Pucyk, P. Radcliffe, H. Redlin, K. Rehlich, M. Richter, M. Roehrs, J. Roensch, R. Romaniuk, M. Ross, J. Rossbach, V. Rybnikov, M. Sachwitz, E. L. Saldin, W. Sandner, H. Schlarb, B. Schmidt, M. Schmitz, P. Schmüser, J. R. Schneider, E. A. Schneidmiller, S. Schnepp, S. Schreiber, M. Seidel, D. Sertore, A. V. Shabunov, C. Simon, S. Simrock, E. Sombrowski, A. A. Sorokin, P. Spanknebel, R. Spesyvtsev, L. Staykov, B. Steffen, F. Stephan, F. Stulle, H. Thom, K. Tiedtke, M.

#222072 - $15.00 USD Received 29 Aug 2014; revised 13 Oct 2014; accepted 14 Oct 2014; published 24 Nov 2014

Tischer, S. Toleikis, R. Treusch, D. Trines, I. Tsakov, E. Vogel, T. Weiland, H. Weise, M. Wellhöfer, M. Wendt, I. Will, A. Winter, K. Wittenburg, W. Wurth, P. Yeates, M. V. Yurkov, I. Zagorodnov, and K. Zapfe, "Operation of a free-electron laser from the extreme ultraviolet to the water window," Nat. Photonics **1**(6), 336–342 (2007).
2. P. Emma, R. Akre, J. Arthur, R. Bionta, C. Bostedt, J. Bozek, A. Brachmann, P. Bucksbaum, R. Coffee, F.-J. Decker, Y. Ding, D. Dowell, S. Edstrom, A. Fisher, J. Frisch, S. Gilevich, J. Hastings, G. Hays, Ph. Hering, Z. Huang, R. Iverson, H. Loos, M. Messerschmidt, A. Miahnahri, S. Moeller, H.-D. Nuhn, G. Pile, D. Ratner, J. Rzepiela, D. Schultz, T. Smith, P. Stefan, H. Tompkins, J. Turner, J. Welch, W. White, J. Wu, G. Yocky, and J. Galayda, "First lasing and operation of an ångstrom-wavelength free-electron laser," Nat. Photonics **4**(9), 641–647 (2010).
3. T. Ishikawa, H. Aoyagi, T. Asaka, Y. Asano, N. Azumi, T. Bizen, H. Ego, K. Fukami, T. Fukui, Y. Furukawa, S. Goto, H. Hanaki, T. Hara, T. Hasegawa, T. Hatsui, A. Higashiya, T. Hirono, N. Hosoda, M. Ishii, T. Inagaki, Y. Inubushi, T. Itoga, Y. Joti, M. Kago, T. Kameshima, H. Kimura, Y. Kirihara, A. Kiyomichi, T. Kobayashi, C. Kondo, T. Kudo, H. Maesaka, X. M. Maréchal, T. Masuda, S. Matsubara, T. Matsumoto, T. Matsushita, S. Matsui, M. Nagasono, N. Nariyama, H. Ohashi, T. Ohata, T. Ohshima, S. Ono, Y. Otake, C. Saji, T. Sakurai, T. Sato, K. Sawada, T. Seike, K. Shirasawa, T. Sugimoto, S. Suzuki, S. Takahashi, H. Takebe, K. Takeshita, K. Tamasaku, H. Tanaka, R. Tanaka, T. Tanaka, T. Togashi, K. Togawa, A. Tokuhisa, H. Tomizawa, K. Tono, S. Wu, M. Yabashi, M. Yamaga, A. Yamashita, K. Yanagida, C. Zhang, T. Shintake, H. Kitamura, and N. Kumagai, "A compact X-ray free-electron laser emitting in the sub-ångström region," Nat. Photonics **6**(8), 540–544 (2012).
4. E. Allaria, R. Appio, L. Badano, W. A. Barletta, S. Bassanese, S. G. Biedron, A. Borga, E. Busetto, D. Castronovo, P. Cinquegrana, S. Cleva, D. Cocco, M. Cornacchia, P. Craievich, I. Cudin, G. D'Auria, M. Dal Forno, M. B. Danailov, R. De Monte, G. De Ninno, P. Delgiusto, A. Demidovich, S. Di Mitri, B. Diviacco, A. Fabris, R. Fabris, W. Fawley, M. Ferianis, E. Ferrari, S. Ferry, L. Froehlich, P. Furlan, G. Gaio, F. Gelmetti, L. Giannessi, M. Giannini, R. Gobessi, R. Ivanov, E. Karantzoulis, M. Lonza, A. Lutman, B. Mahieu, M. Milloch, S. V. Milton, M. Musardo, I. Nikolov, S. Noe, F. Parmigiani, G. Penco, M. Petronio, L. Pivetta, M. Predonzani, F. Rossi, L. Rumiz, A. Salom, C. Scafuri, C. Serpico, P. Sigalotti, S. Spampinati, C. Spezzani, M. Svandrlik, C. Svetina, S. Tazzari, M. Trovo, R. Umer, A. Vascotto, M. Veronese, R. Visintini, M. Zaccaria, D. Zangrando, and M. Zangrando, "Highly coherent and stable pulses from the FERMI seeded free-electron laser in the extreme ultraviolet," Nat. Photonics **6**(10), 699–704 (2012).
5. R. Xu, H. Jiang, C. Song, J. A. Rodriguez, Z. Huang, C.-C. Chen, D. Nam, J. Park, M. Gallagher-Jones, S. Kim, S. Kim, A. Suzuki, Y. Takayama, T. Oroguchi, Y. Takahashi, J. Fan, Y. Zou, T. Hatsui, Y. Inubushi, T. Kameshima, K. Yonekura, K. Tono, T. Togashi, T. Sato, M. Yamamoto, M. Nakasako, M. Yabashi, T. Ishikawa, and J. Miao, "Single-shot three-dimensional structure determination of nanocrystals with femtosecond X-ray free-electron laser pulses," Nat. Commun. **5**, 4061 (2014).
6. H. N. Chapman, A. Barty, M. J. Bogan, S. Boutet, M. Frank, S. P. Hau-Riege, S. Marchesini, B. W. Woods, S. Bajt, W. Henry Benner, R. A. London, E. Plönjes, M. Kuhlmann, R. Treusch, S. Düsterer, T. Tschentscher, J. R. Schneider, E. Spiller, T. Möller, C. Bostedt, M. Hoener, D. A. Shapiro, K. O. Hodgson, D. Van Der Spoel, F. Burmeister, M. Bergh, C. Caleman, G. Huldt, M. Marvin Seibert, F. R. N. C. Maia, R. W. Lee, A. Szöke, N. Timneanu, and J. Hajdu, "Femtosecond diffractive imaging with a soft-X-ray free-electron laser," Nat. Phys. **2**(12), 839–843 (2006).
7. I. K. Robinson, I. A. Vartanyants, G. J. Williams, M. A. Pfeifer, and J. A. Pitney, "Reconstruction of the Shapes of Gold Nanocrystals Using Coherent X-Ray Diffraction," Phys. Rev. Lett. **87**(19), 195505 (2001).
8. M. A. Pfeifer, G. J. Williams, I. A. Vartanyants, R. Harder, and I. K. Robinson, "Three-dimensional mapping of a deformation field inside a nanocrystal," Nature **442**(7098), 63–66 (2006).
9. D. Shapiro, P. Thibault, T. Beetz, V. Elser, M. Howells, C. Jacobsen, J. Kirz, E. Lima, H. Miao, A. M. Neiman, and D. Sayre, "Biological imaging by soft x-ray diffraction microscopy," Proc. Natl. Acad. Sci. U.S.A. **102**(43), 15343–15346 (2005).
10. K. J. Gaffney and H. N. Chapman, "Imaging atomic structure and dynamics with ultrafast x-ray scattering," Science **316**(5830), 1444–1448 (2007).
11. R. Bonifacio, C. Pellegrini, and L. M. Narducci, "Collective instabilities and high-gain regime in a free electron laser," Opt. Commun. **50**(6), 373–378 (1984).
12. E. L. Saldin, E. A. Schneidmiller, and M. V. Yurkov, "Statistical properties of radiation from VUV and X-ray free electron laser," Opt. Commun. **148**(4-6), 383–403 (1998).
13. G. Dattoli, A. Marino, A. Renieri, and F. Romanelli, "Hamiltonian Picture of a Free Electron Laser," IEEE J. Quantum Electron. **17**(8), 1371–1387 (1981).
14. R. Ischebeck, J. Feldhaus, Ch. Gerth, E. Saldin, P. Schmüser, E. Schneidmiller, B. Steeg, K. Tiedtke, M. Tonutti, R. Treusch, and M. Yurkov, "Study of the transverse coherence at the TTF free electron laser," Nucl. Instrum. Methods Phys. Res. A **507**(1-2), 175–180 (2003).
15. A. Singer, I. A. Vartanyants, M. Kuhlmann, S. Duesterer, R. Treusch, and J. Feldhaus, "Transverse-Coherence Properties of the Free-Electron-Laser FLASH at DESY," Phys. Rev. Lett. **101**(25), 254801 (2008).
16. A. Singer, U. Lorenz, F. Sorgenfrei, N. Gerasimova, J. Gulden, O. M. Yefanov, R. P. Kurta, A. Shabalin, R. Dronyak, R. Treusch, V. Kocharyan, E. Weckert, W. Wurth, and I. A. Vartanyants, "Hanbury Brown-Twiss Interferometry at a Free-Electron Laser," Phys. Rev. Lett. **111**(3), 034802 (2013).
17. P. Mercere, R. Bachelard, M. E. Couprie, M. Idir, S. Bucourt, G. Dovillaire, X. Levecq, O.V. Chubar, J. Gautier, G. Lambert, P. Zeitoun, T. Hara, A. Higashiya, T. Ishikawa, M. Nagasono, M. Yabashi, H. Kimura, H. Ohashi,

#222072 - $15.00 USD Received 29 Aug 2014; revised 13 Oct 2014; accepted 14 Oct 2014; published 24 Nov 2014

"SPATIAL CHARACTERIZATION OF SASE-FEL OF SCSS TEST ACCELERATOR" in 2009 FEL International Conferece (Liverpool), pg. 72 (2009).
18. R. Bachelard, P. Mercère, M. Idir, M.-E. Couprie, M. Labat, O. Chubar, G. Lambert, Ph. Zeitoun, H. Kimura, H. Ohashi, A. Higashiya, M. Yabashi, M. Nagasono, T. Hara, and T. Ishikawa, "Wavefront Analysis of Nonlinear Self-Amplified Spontaneous-Emission Free-Electron Laser Harmonics in the Single-Shot Regime," Phys. Rev. Lett. **106**(23), 234801 (2011).
19. B. Flöter, P. Juranić, S. Kapitzki, B. Keitel, K. Mann, E. Plönjes, B. Schäfer, and K. Tiedtke, "EUV Hartmann sensor for wavefront measurements at the Free-electron LASer in Hamburg," New J. Phys. **12**(8), 083015 (2010).
20. B. Schäfer, B. Flöter, T. Mey, P. Juranic, S. Kapitzki, B. Keitel, E. Plönjes, K. Mann, and K. Tiedtke, "FEL beam characterization from measurements of the Wigner distribution function," Nucl. Instrum. Methods Phys. Res. A **654**(1), 502–507 (2011).
21. L. Raimondi, C. Svetina, N. Mahne, D. Cocco, F. Capotondi, E. Pedersoli, M. Kiskinova, B. Keitel, G. Brenner, E. Plönjes, T. Mey, K. Mann, M. Zangrando Proc. SPIE 8848, Advances in X-Ray/EUV Optics and Components VIII, 88480B (2013).
22. H. J. Park, N. D. Loh, R. G. Sierra, C. Y. Hampton, D. Starodub, A. V. Martin, A. Barty, A. Aquila, J. Schulz, J. Steinbrener, R. L. Shoeman, L. Lomb, S. Kassemeyer, C. Bostedt, J. Bozek, S. W. Epp, B. Erk, R. Hartmann, D. Rolles, A. Rudenko, B. Rudek, L. Foucar, N. Kimmel, G. Weidenspointner, G. Hauser, P. Holl, E. Pedersoli, M. Liang, M. S. Hunter, L. Gumprecht, N. Coppola, C. Wunderer, H. Graafsma, F. R. N. C. Maia, T. Ekeberg, M. Hantke, H. Fleckenstein, H. Hirsemann, K. Nass, H. J. Tobias, G. R. Farquar, W. H. Benner, S. Hau-Riege, C. Reich, A. Hartmann, H. Soltau, S. Marchesini, S. Bajt, M. Barthelmess, L. Strueder, J. Ullrich, P. Bucksbaum, M. Frank, I. Schlichting, H. N. Chapman, M. J. Bogan, and V. Elser, "Toward unsupervised single-shot diffractive imaging of heterogeneous particles using X-ray free-electron lasers," Opt. Express **21**(23), 28729–28742 (2013).
23. C. Gutt, P. Wochner, B. Fischer, H. Conrad, M. Castro-Colin, S. Lee, F. Lehmkühler, I. Steinke, M. Sprung, W. Roseker, D. Zhu, H. Lemke, S. Bogle, P. H. Fuoss, G. B. Stephenson, M. Cammarata, D. M. Fritz, A. Robert, and G. Grübel, "Single Shot Spatial and Temporal Coherence Properties of the SLAC Linac Coherent Light Source in the Hard X-Ray Regime," Phys. Rev. Lett. **108**(2), 024801 (2012).
24. M. D. Alaimo, M. A. C. Potenza, M. Manfredda, G. Geloni, M. Sztucki, T. Narayanan, and M. Giglio, "Probing the Transverse Coherence of an Undulator X-Ray Beam Using Brownian Particles," Phys. Rev. Lett. **103**(19), 194805 (2009).
25. M. Ferrario, D. Alesini, M. Anania, A. Bacci, M. Bellaveglia, O. Bogdanov, R. Boni, M. Castellano, E. Chiadroni, A. Cianchi, S. B. Dabagova, C. De Martinis, D. Di Giovenale, G. Di Pirro, U. Dosselli, A. Drago, A. Esposito, R. Faccini, A. Gallo, M. Gambaccini, C. Gatti, G. Gatti, A. Ghigo, D. Giulietti, A. Ligidov, P. Londrillo, S. Lupi, A. Mostacci, E. Pace, L. Palumbo, V. Petrillo, R. Pompili, A. R. Rossi, L. Serafini, B. Spataro, P. Tomassini, G. Turchetti, C. Vaccarezza, F. Villa, G. Dattoli, E. Di Palma, and L. Giannessi, "SPARC_LAB present and future," Nucl. Instrum. Methods Phys. Res. B **309**, 183–188 (2013).
26. L. Giannessi, D. Alesini, P. Antici, A. Bacci, M. Bellaveglia, R. Boni, M. Boscolo, F. Briquez, M. Castellano, L. Catani, E. Chiadroni, A. Cianchi, F. Ciocci, A. Clozza, M. E. Couprie, L. Cultrera, G. Dattoli, M. Delfranco, A. Dipace, G. Dipirro, A. Doria, A. Drago, W. F. Fauley, M. Ferrario, L. Ficcadenti, D. Filippetto, F. Frassetto, H. P. Freund, V. Fusco, G. Gallerano, A. Gallo, G. Gatti, A. Ghhigo, E. Giovenale, A. Marinelli, M. Labat, B. Marchetti, G. Marcus, C. Marelli, M. Mattioli, M. Migliorati, M. Moreno, A. Mostacci, G. Orlandi, E. Pace, L. Palumbo, A. Petralia, M. Petrarca, V. Petrillo, L. Poletto, M. Quattromini, J. V. Rau, S. Reiche, C. Ronsivalle, J. Rosenzweig, A. R. Rossi, V. Rossi Albertini, E. Sabia, L. Serafini, M. Serluca, I. Spassovsky, B. Spataro, V. Surrenti, C. Vaccarezza, M. Vescovi, and C. Vicario, "Self-Amplified Spontaneous emission for a single pass Free-Electron Laser," Phys. Rev. ST Acc. Beams **14**(6), 060712 (2011).
27. J. W. Goodman, *Statistical Optics* (Wiley Classical Library 2000).
28. M. A. C. Potenza, K. P. V. Sabareesh, M. Carpineti, M. D. Alaimo, and M. Giglio, "How to Measure the Optical Thickness of Scattering Particles from the Phase Delay of Scattered Waves: Application to Turbid Samples," Phys. Rev. Lett. **105**(19), 193901 (2010).
29. S. Mazzoni, M. A. C. Potenza, M. D. Alaimo, S. J. Veen, M. Dielissen, E. Leussink, J.-L. Dewandel, O. Minster, E. Kufner, G. Wegdam, and P. Schall, "SODI-COLLOID: A combination of static and dynamic light scattering on board the International Space Station," Rev. Sci. Instrum. **84**(4), 043704 (2013).
30. M. Quattromini, M. Artioli, E. Di Palma, A. Petralia, and L. Giannessi, "Focusing properties of linear undulators," Phys. Rev. ST Accel. Beams **15**(8), 080704 (2012).
31. L. Poletto, S. Bonora, M. Pascolini, and P. Villoresi, "Instrumentation for analysis and utilization of estreme-ultraviolet and soft X-ray high-order harmonics," Rev. Sci. Instrum. **75**(11), 4413 (2004).
32. H. C. van de Hulst, *Light Scattering by Small Particles* (John Wiley and Sons 1957).
33. E. L. Saldin, E. A. Schneidmiller, and M. V. Yurkov, "Output power and degree of transverse coherence of X-ray free electron lasers," Opt. Commun. **281**(18), 4727–4734 (2008).
34. G. Geloni, E. Saldin, L. Samoylova, E. Schneidmiller, H. Sinn, Th. Tschentscher, and M. Yurkov, "Coherence properties of the European XFEL," New J. Phys. **12**(3), 035021 (2010).
35. S. Reiche, "GENESIS 1.3: a fully 3D time-dependent FEL simulation code," Nucl. Instrum. Methods Phys. Res. A **429**(1-3), 243–248 (1999).

#222072 - $15.00 USD Received 29 Aug 2014; revised 13 Oct 2014; accepted 14 Oct 2014; published 24 Nov 2014

1. Introduction

Free Electron Lasers (FELs) user facilities [1–4] have become a widespread reality, as witnessed by the recent commissioning of light sources which satisfy the increasingly demanding requirement in terms of beam quality and tunability. In particular, the high degree of spatial coherence is a capital asset for FELs, which are envisioned to provide a powerful tool for some of the most promising methods in the investigation of nanostructured [5, 6], inorganic [7, 8] and organic [9] systems, requiring a coherent irradiation of the sample with a large flux of high energy photons. The FEL radiation mechanism is based on the interaction between a relativistic electron beam wiggling in a periodic magnetic field and an electromagnetic radiation field [10], that in the Self Amplified Spontaneous Emission (SASE) operating mode is the spontaneous undulator emission. In this regime, the radiation starts from noise and its intensity grows exponentially along the undulator [11–13], with a correspondent enhancement of longitudinal and transverse coherence. The characterization of transverse coherence properties is universally recognized to be critical both for the correct assessment of the operating conditions of the machine and for the data analysis. The most commonly used techniques are based on Young's [14, 15] or Hanbury Brown-Twiss's [16] interferometers and rely on the use of a large number of shots in order to gauge the coherence over the scale lengths of interest. Data coming from different radiation pulses are merged together, losing any possibly attractive information coming from a statistical analysis. Wavefront analysis using Hartmann Wavefront Sensors was proposed to determine the spatial characteristics of the FEL source in single-shot regime [17] and demonstrated at the SCSS Test Accelerator [18], at FLASH [19,20] and at FERMI [21]. At LCLS, besides the study about the wavefront [22], an evaluation of the transverse coherence in the X ray range has been performed by measuring the homodyne speckle intensity due to coherent diffraction by disordered samples in the low and wide angle configurations [23], paving the way for the application of statistical methods on FELs.

A new method for probing the transverse coherence, particularly appealing for its simplicity and data finesse, was described in [24]. It is based on the statistical analysis of the speckle field produced by heterodyning the test beam with a huge number of reference waves generated via scattering by a suspension of particles.

In this paper, we propose a generalization of the aforementioned method for measuring the two-dimensional single-shot transverse coherence that overcomes the limitations imposed by extended coherence area. We exploit for the first time this generalized method to the case of FEL radiation. Measurements were performed at the SPARC-LAB test facility [25,26] and were addressed to extend the speckle technique to cases where the coherence area is comparable to the beam size, a situation substantially different with respect to the previous application of the speckle analysis to the synchrotron light discussed in [24]. Moreover, we monitored the evolution of the transverse coherence of the FEL radiation along the undulator modules.

The plan of the work is the following: in Section 1, we present the theoretical considerations at the basis of the speckle technique; in Section 2, we describe the experimental set up of the diagnostics and the properties of the FEL electron beam and radiation. In Section 3, the collected data are shown and analyzed. Conclusions and comments close the paper.

2. Speckle technique for the transverse coherence measure, theoretical considerations

Speckles are produced by illuminating with a field E_0 a collection of randomly distributed scatterers. They are detected by recording the intensity distribution in points of transverse coordinates **r** by means of a CCD camera placed at a distance z from the sample, along the optical axis. The i^{th} particle scatters an almost spherical wave E_{si} that interferes with the transmitted beam, generating a circular fringe system, as shown in Fig. 1. The visibility of the

#222072 - $15.00 USD Received 29 Aug 2014; revised 13 Oct 2014; accepted 14 Oct 2014; published 24 Nov 2014

fringes as function of the distance $\Delta\mathbf{r} = \mathbf{r}\text{-}\mathbf{r}_i$ from the particle center $\mathbf{r}_i$ [27] is connected to the modulus of the Mutual Intensity Function (MIF):

$$J(\mathbf{r}_i, \mathbf{r}_i + \Delta\mathbf{r}) = \left\langle E_0(\mathbf{r}_i) E_0{}^*(\mathbf{r}_i + \Delta\mathbf{r}) \right\rangle \tag{1}$$

<...> indicating the average over the statistical ensemble of field realizations [28] coinciding, in the hypothesis of ergodicity, with the temporal average.

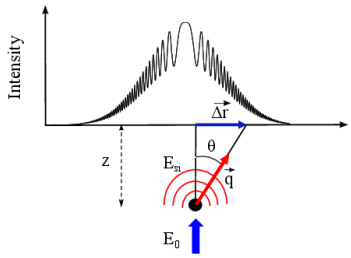

Fig. 1. Geometry of the system where θ is the scattering angle and **q** the direction of the scattered wave.

In presence of N randomly distributed particles, the intensity recorded by the sensor is given by:

$$I(\mathbf{r}) = \left|E_0\right|^2 + 2\,\mathrm{Re}(E_0 E_s{}^*) \tag{2}$$

where $E_s = \sum_{i=1}^{N} E_{si}$ and the term $|E_s|^2$ was neglected for weakly scattering samples. The term proportional to E_s represents the heterodyne signal and, according to [24], the spatial Power Spectrum $S(\mathbf{q})$ of the heterodyne speckles turns out to be proportional to the sum of the squared MIFs

$$\left|\tilde{J}(\Delta\mathbf{r})\right|^2 = \sum_{i=1}^{N} \left|J(\mathbf{r}_i, \mathbf{r}_i + \Delta\mathbf{r})\right|^2 \tag{3}$$

produced by all the particles across the beam section. The dependence is just on $\Delta\mathbf{r}$ because the Power Spectrum (PS), while retaining the information about the intensity rms fluctuations (fringe visibility), loses the information about phase, connected to the particle positions. Substantial data reduction is required for getting $\tilde{J}(\Delta\mathbf{r})$. Once that the heterodyne signal is purged by the background, $S(\mathbf{q})$ can be written as a function of the scattering wave vector $\mathbf{q} = 2k\sin(\theta/2)\mathbf{e}_q$:

$$S(\mathbf{q}) = \left|J(\mathbf{q})\right|^2 F(\mathbf{q}) T(\mathbf{q}) + K(\mathbf{q}) \tag{4}$$

after having operated the rescaling $\Delta r = zq/k$, with $k = 2\pi/\lambda$, θ the scattering angle and $\mathbf{e}_q$ the wave vector direction. $F(\mathbf{q})$ is the scatterer form factor (chosen as broader as possible), $T(\mathbf{q})$ is the Talbot transfer function [29] and $K(\mathbf{q})$ is the shot noise contribution. .

3. Experimental set up

The speckle detection at SPARC_LAB was performed in two different shifts with similar electron beams and working points. The SPARC FEL was driven by an electron bunch produced by the photoinjector, accelerated in the linac to a final electron energy E_B = 162.5

#222072 - $15.00 USD Received 29 Aug 2014; revised 13 Oct 2014; accepted 14 Oct 2014; published 24 Nov 2014

MeV (corresponding to an electron Lorentz factor γ≈335 and then matched to the undulator system (6 sections, with movable gaps, of 75 periods λ = 2.8 cm) [30].

Table 1. Main electron beam parameter

Quantity	value
Beam energy E_B(MeV)	162.5 ± 0.27
Beam charge (pC)	312 ± 16
Energy Spread (projected %)	0.2 ± 0.015
Energy Spread (slice %)	0.050 ± 0.005
Length r.m.s. (ps)	1.65 ± 0.05
Beam current Ipeak(A)	75.63 ± 3.5
Vertical Emittance 90% (mmmrad)	1.95 ± 1.0
Horizontal Emittance 90%(mmmrad)	1.74 ± 1.1

The undulator was tuned at the resonant wavelength $\lambda = \frac{\lambda_u (1 + K^2/2)}{2\gamma^2} = 402\,nm$, K being the deflecting parameter of the undulator. The main parameters of the electron beam are listed in Table 1. Light was collected downstream the undulator, progressively

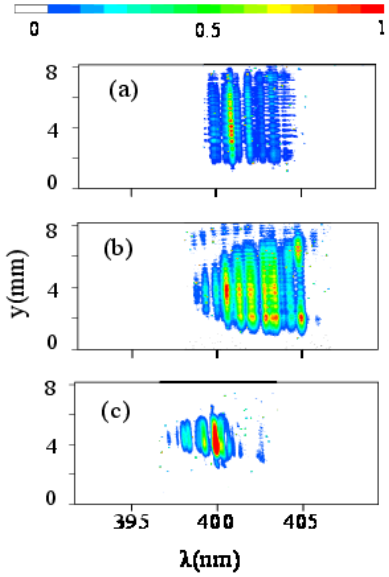

Fig. 2. Energy spectra after the 4th (a), 5th (b) and 6th (c) undulator. The vertical axis in each picture indicates the position on the vertical entrance slit of the spectrometer. Spectrometer Luxor with a CCD detector (Versarray, 1300B-Princeton Instruments).

activating the 4th, 5th and 6th section, and was sent alternately to the speckle apparatus and to the spectrometer [31]. Typical energy spectra are shown in Fig. 2, while the experimental and simulated growth of the FEL radiation is presented in Fig. 3. The radiation energy values are summarized in Table 2.

#222072 - $15.00 USD Received 29 Aug 2014; revised 13 Oct 2014; accepted 14 Oct 2014; published 24 Nov 2014

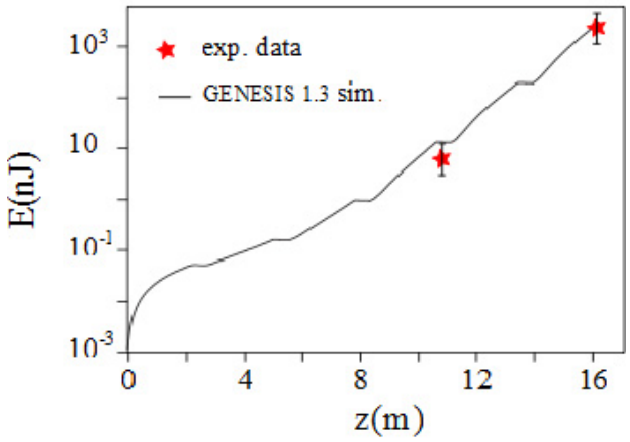

Fig. 3. Experimental and simulated energy growth as a function of the undulator length z (m). Beam parameters in Table 1.

The speckle diagnostics was based on a low concentrated suspension (0.3% w/w) of calibrated polystyrene spheres with index of refraction n = 1.63 at wavelength 402 nm, and a diameter of 2.1 μm, filled in a glass cuvette 2 mm thick. Given the radius of the scatters, the particle form factor F(**q**) can be evaluated according to the Mie's solution of the Maxwell equations [32], and was found to vary from 1 to 0.92 over the accessible **q** range.

Table 2. Measured and simulated radiation properties

Sections	4u	5u	6u
Energy (experimental)	5.4 ± 2.8 nJ	-	2.4 ± 1.9 μJ
Energy (simulated)	11 nJ	156 nJ	2.2 μJ

The working distance z was chosen in such a way that the speckles are properly resolved, viz., $z \geq z_{\lim} = 2\pi l_c / (\lambda q_{\max})$, being q_{max} the detector resolution and l_c the coherent size, that in cases where the of large coherence approaches the beam dimension. We used a 14-bit CCD camera PCO1600 of 1200x1200 resolution and pixel size 7.4 μm, placed at z = 130 mm .

4. Data analysis

The raw intensity distribution of the beam I is presented in Fig. 4(a). The tiny speckle structure is hardly noticeable, being almost entirely overwhelmed by the coarse and sharp structures of the intensity $|E_0|^2$ of the test beam itself. However, while coarser structures exhibit large shot-to-shot variations related to the SASE statistics, fine structures show small shot-to-shot variations, due to the slow diffusive or convective dynamics of particles in solution. This allows to distinguish the scattering signal from any other straylight contribution introduced by the test beam by taking a lower-limit cut-off spatial filtering ($q>0.15\mu m^{-1}$). The corresponding high-pass filtered intensity distribution is

#222072 - $15.00 USD Received 29 Aug 2014; revised 13 Oct 2014; accepted 14 Oct 2014; published 24 Nov 2014

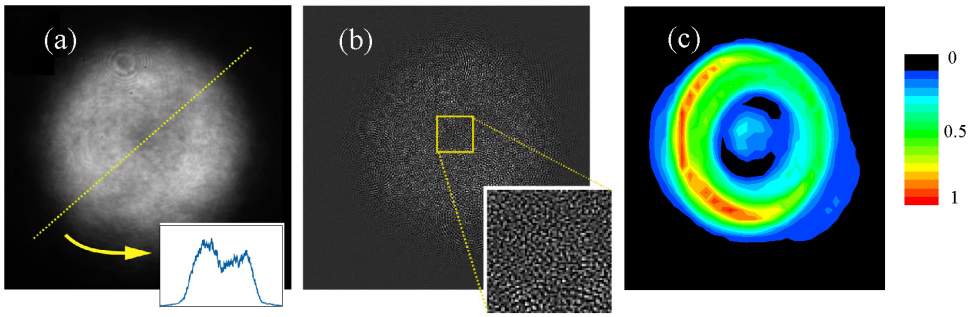

Fig. 4. (a) FEL intensity distribution I(**r**) after 6 undulators. In the inset, radial profile of the intensity. (b) Speckle contained in (a) after a lower-limit cut-off spatial filtering. (c) Radiation power given by GENESIS 1.3 simulation at the end of the undulator.

shown in Fig. 4(b), where the speckle structure becomes evident. The quantitative characterization of the speckle statistics is then performed by Fourier transforming the signal and by analyzing the intensity power spectra. Figure 5(a) shows the raw PS of the intensity distribution of Fig. 4(a).

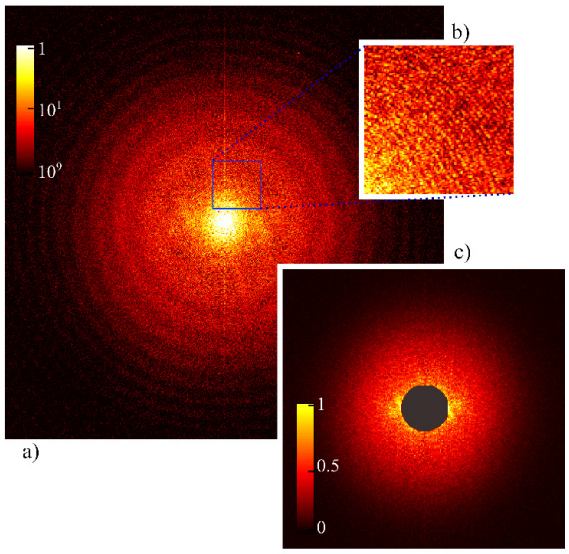

Fig. 5. (a) Power spectrum S(**q**) relevant to the case of Fig. 3. (b) Detail of S(**q**) showing the Talbot oscillation. (c) Modulus of the Mutual Intensity Function.

As far as fine details are concerned, two distinct oscillatory behaviors due to the Talbot Transfer Function T(**q**) can be observed. Fast oscillations (see inset (b)) have positions assigned by z equal to the working distance, and are essentially due to the scattering from silica particles. Conversely, slow oscillations, whose positions are assigned by a distance z≈4 mm corresponding to the casing between the CCD and the front-end glass, can be attributed to the parasitic scattering from dust particles attracted to the camera glass, likely because of long exposure to ionizing radiation. Such a contribution could be removed either by averaging the oscillations, or by taking the PS of the difference between the acquired image and a reference image, both normalized to the same average intensity. We found the latter approach to be

#222072 - $15.00 USD Received 29 Aug 2014; revised 13 Oct 2014; accepted 14 Oct 2014; published 24 Nov 2014

robust enough even if the illuminating intensity distribution of the two images exhibits the typical shot-to-shot fluctuations of the SASE radiation. The Power Spectrum was indeed completely dictated by speckles statistics for $q \geq 0.15\ \mu m^{-1}$, corresponding to $\Delta r \geq 1mm$. A typical 2D single-shot MIF map is shown in Fig. 5(c), where the inner part of the distribution for $q<0.15\ \mu m^{-1}$ has not been reported. It appears to be isotropic and the average respect to the azimuthal angle $\left\langle \left|\tilde{J}\right|^2 \right\rangle_a$ is plotted in Fig. 6 (the data are taken from the first shift) for four, five and six active undulator sections, respectively, together with the corresponding intensity autocorrelation $A_I(\Delta\mathbf{r}) = \langle I(\mathbf{r}) I(\mathbf{r}+\Delta\mathbf{r}) \rangle$. In all three cases, $\left\langle \left|\tilde{J}\right|^2 \right\rangle_a$ for $|\Delta\mathbf{r}|>1mm$ is well described by gaussian distributions with rms values $\sigma_{4u} = 1.8$ mm, $\sigma_{5u} = 1.4$ mm, $\sigma_{6u} = 1.3$mm.

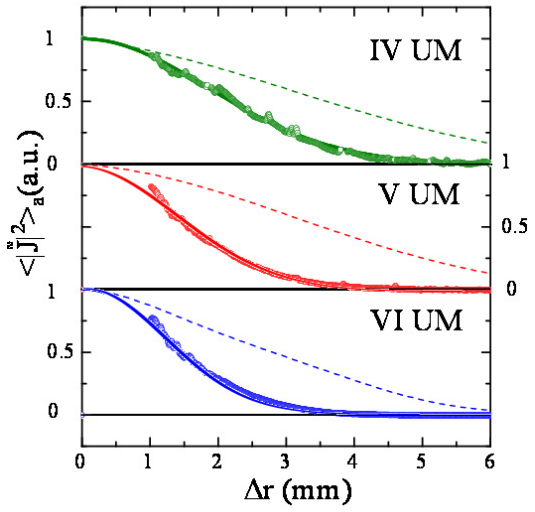

Fig. 6. Angular average of the squared MIF $\left\langle \left|\tilde{J}\right|^2 \right\rangle_a$ measured after the 4th, 5th and 6th sections (open circles: experiments, solid: Gaussian fit) and beam intensity autocorrelation function (dashed).

Thanks to the heterodyne, and contrarily to the case of homodyne measurements, both $\tilde{J}(\Delta\mathbf{r})$ and the beam intensity autocorrelation $A_I(\Delta\mathbf{r})$ are deduced by the same image, the high spatial frequencies (speckles) mostly affecting the former and the low spatial frequencies (coarse intensity distribution) the latter. In the Complex Coherence Function [34,35]

$$\gamma = \frac{\tilde{J}(\Delta\mathbf{r})}{\sqrt{\langle I(\mathbf{r}) I(\mathbf{r}+\Delta\mathbf{r}) \rangle}}, \tag{5}$$

the normalization with respect to $\sqrt{A_I(\Delta\mathbf{r})}$ permits to generalize the coherence factor to cases where the coherence area is of the order of the beam size, accounting for the inhomogeneities at the probing points. It allows to express the information about coherence by means of a single scalar value, the degree of coherence:

$$\zeta = \frac{\int \left|\tilde{J}(\Delta\mathbf{r})\right|^2 d\Delta\mathbf{r}}{\int \left|A_I(\Delta\mathbf{r})\right|^2 d\Delta\mathbf{r}}. \tag{6}$$

#222072 - $15.00 USD Received 29 Aug 2014; revised 13 Oct 2014; accepted 14 Oct 2014; published 24 Nov 2014

Experimental values of ζ for both shifts (blue squared for the first and red squared for the second) are plotted in Fig. 7.

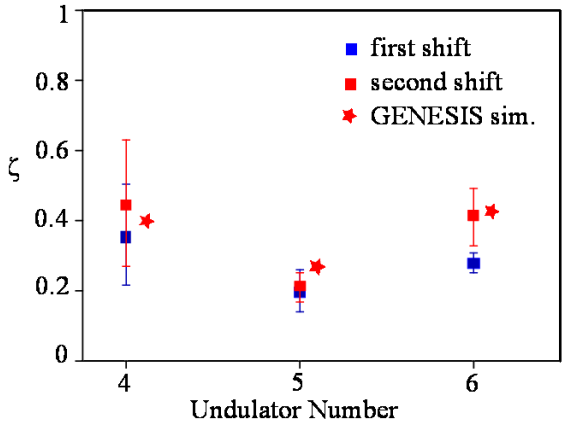

Fig. 7. Angular average of the squared MIF measured after the 4th, 5th and 6th sections (open circles: experiments, solid: Gaussian fit) and beam intensity autocorrelation function (dashed).

The experimental measures of the transverse coherence present relatively large values at the 4th section, a slight drop at the 5th and a further increase at the end of the undulator to sizable values. The analysis of the spectra of Fig. 2 and the increase of the radiation intensity given in Fig. 3 and Table 2 indicate that the system is in the exponential phase of the emission, the e-beam reaching the end of the undulator before the radiation saturation. The FEL was optimized for maximum energy pulse output, corresponding to a detuned resonance in the last undulators. The value of the undulator parameter of the last two sections was decreased by about 3%. This taper was affecting the mode quality. The resonance condition was indeed verified off-axis and the radiation pulse presented a central depression, visible in Fig. 4(a) and retrieved in the relevant simulations (Fig. 4(c)), that were done with values of the deflecting parameters K of the last undulators used in the experiment and lower by a few percents with respect to the case corresponding to the ideal matching. The presence of the first mode TEM_{01}, giving a typical donut shape to the output beam, can be recognized. Furthermore, the theoretical estimates of ζ obtained from Eq. (6) using simulations performed with the code GENESIS 1.3 with beam parameters similar to the measured ones are reported in Fig. 7 (red stars). The deviation from a transverse gaussian distributions, taking place when the beam is constituted by more transverse modes, concur to lower the coherence. The agreement of these values with the experimental data is quite good. Some comments on possible sources of uncertainty on the measurements are in order. The light collection from different positions along the undulator was not done exactly with the same geometry. In the acquisition from the 4th undulator, the beam size was close to the CCD size, determining a small artificial clipping of the beam. In addition, the radiation pulse obtained with four active undulators was vertically cut by the edges of vacuum chamber itself, as suggested by the y distribution of the spectral intensity, reported on ordinate in Fig. 2(a). The presence of horizontal interference fringes introduces a variation in the shape of the incoming beam, resulting in a slight error in the determination of the FEL beam properties.

Conclusions

In conclusion, we have presented the application of the speckle technique to the measure of the transverse coherence of a SASE FEL radiation. The heterodyne configuration allows the

#222072 - $15.00 USD Received 29 Aug 2014; revised 13 Oct 2014; accepted 14 Oct 2014; published 24 Nov 2014

simultaneous acquisition of both the scattering signal and FEL beam intensity distribution. The rigorous data normalization, necessary for the case of FEL sources, which are expected to exhibit a large degree of coherence, requires full information about the intensity distribution, contrarily to the case of the synchrotron radiation, where the broad intensity distribution is slowly varying over the small coherence area and can be considered uniform. In our case, the measurement method was demonstrated to be precise and robust, permitting insight into the radiation physics. It does not require any a priori assumptions and can be implemented over a wide range of wavelengths, from the optical radiation to the x-rays.

Acknowledgments

The authors gratefully acknowledge Proff. M. Giglio and G. Geloni for their interest and support and the whole SPARC Team for long hours spent in the control room for making this experiment possible. The work has been partially supported by the Italian Minister of Research in the framework of FIRB- Fondo per gli Investimenti della Ricerca di Base, Project n. RBFR12NK5K.

#222072 - $15.00 USD Received 29 Aug 2014; revised 13 Oct 2014; accepted 14 Oct 2014; published 24 Nov 2014